Electrical Measurements of Bilayer Membranes Formed by Langmuir−Blodgett Deposition on Single-Crystal Silicon

ARTICLE *in* LANGMUIR · JANUARY 2008

Impact Factor: 4.46 · DOI: 10.1021/la702147m · Source: PubMed

5 AUTHORS, INCLUDING:

Mikhail Merzlyakov
Johns Hopkins University
62 PUBLICATIONS **1,085** CITATIONS
SEE PROFILE

Peter Searson
Johns Hopkins University
297 PUBLICATIONS **11,822** CITATIONS
SEE PROFILE

Electrical Measurements of Bilayer Membranes Formed by Langmuir−Blodgett Deposition on Single-Crystal Silicon

Vesselin Nikolov, Janice Lin, Mikhail Merzlyakov, Kalina Hristova,* and Peter C. Searson*

Department of Materials Science and Engineering, Johns Hopkins University, Baltimore, Maryland 21218

Received July 17, 2007. In Final Form: September 13, 2007

Bilayer membranes on solid supports are used for fundamental studies of biophysical properties and for the development of biosensors and other devices. Here we report on electrically addressable bilayer membranes formed by Langmuir−Blodgett (LB)-based deposition on single-crystal silicon. The incorporation of a polymer cushion ensures high lipid mobility in both the lower and upper leaflet, allowing the potential for combined investigations of electrical, structural, and dynamic characteristics of membrane-associated proteins. Impedance spectroscopy is used to demonstrate that the lipid bilayers are robust and reproducible with an impedance of about 10^4 Ω cm^2 and a capacitance of about 0.8 μF cm^{-2}. The ability to characterize ion channels is demonstrated using the model system gramicidin. These results demonstrate that artificial bilayers formed by LB deposition have many unique advantages for electrical measurements of membranes and their components.

Introduction

Artificial bilayer membranes on solid supports are platforms for fundamental research and technological applications.[1] Two approaches, based on self-assembly, are currently used to produce surface-supported bilayers: vesicle fusion, in which vesicles break and self-assemble into bilayers on a solid support,[2−7] and chemical tethering/vesicle fusion, in which the membrane architecture is formed by first chemically binding some or all of the lower leaflet to the solid support, usually exploiting gold/thiol self-assembled monolayer chemistry, followed by vesicle fusion to form the upper leaflet.[8−16]

The chemical tethering/vesicle fusion approach has several features that are ideal for sensor applications. The covalent binding of the lower leaflet to the support results in very high membrane resistance, typically larger than 10^7 Ω cm^2, and in a large dynamic range for measurements with ion channels. In addition, the tethering results in bilayers that are more robust than traditional black lipid membranes. The vesicle fusion approach can be used to produce supported bilayers; however, significant concentrations of charged lipids and cholesterol are often required to obtain defect-free membranes for electrical measurements. While both tethering/vesicle fusion and vesicle fusion have significant advantages, other approaches are needed to produce biomimetic membranes that mimic the properties of cell membranes. Key features are maintaining mobility of lipids and proteins in the upper and lower leaflet, and the ability to incorporate peptides in the membrane, especially those with flanks that extend beyond the thickness of the membrane.

Recently, bilayers on glass or quartz supports prepared by Langmuir−Blodgett (LB)-based deposition techniques have been developed as alternatives for self-assembled bilayers. In the first step, a monolayer is deposited onto a solid support using LB deposition. The lower leaflet usually incorporates a fraction of lipids modified with a poly(ethylene glycol) group to provide a polymer cushion, thereby ensuring high lipid and protein mobility in upper and lower leaflets. In the second step, the upper leaflet of the bilayer is formed by Langmuir−Schaeffer (LS) deposition or vesicle fusion (VF). LB-based bilayers are excellent model systems since the lateral mobility of lipids and membrane proteins is comparable to values in cell membranes.[17] Furthermore, LB deposition allows control over the concentration and orientation of peptides.[18−22] Fluorescence-based characterization of lipids and proteins in LB bilayers has provided new structural, thermodynamic, and kinetic information about membranes.[18−22] In this paper we use electrochemical impedance spectroscopy to characterize the electrical properties of supported bilayer membranes formed by LB-based deposition on single-crystal silicon. We show that the impedance response of LB bilayers on silicon is reproducible and robust over a wide potential range and can be modeled as a series combination of two parallel RC loops corresponding to the silicon/solution interface and the

* To whom correspondence should be addressed. E-mail: kh@jhu.edu (K.H.); searson@jhu.edu (P.C.S.).

(1) Sackmann, E. *Science* **1996**, *271*, 43−48.
(2) Li, E.; Hristova, K. *Langmuir* **2004**, *20*, 9053−9060.
(3) Stottrup, B. L.; Veatch, S. L.; Keller, S. L. *Biophys. J.* **2004**, *86*, 2942−2950.
(4) Gritsch, S.; Nollert, P.; Jahnig, F.; Sackmann, E. *Langmuir* **1998**, *14*, 3118−3125.
(5) Nikolov, V.; Radisic, A.; Hristova, K.; Searson, P. C. *Langmuir* **2006**, *22*, 7156−7158.
(6) Bartlett, P. N.; Brace, K.; Calvo, E. J.; Etchenique, R. *J. Mater. Chem.* **2000**, *10*, 149−156.
(7) Rossi, C.; Briand, E.; Parot, P.; Odorico, M.; Chopineau, J. *J. Phys. Chem.* B **2007**, *111*, 7567−7576.
(8) Atanasov, V.; Knorr, N.; Duran, R. S.; Ingebrandt, S.; Offenhausser, A.; Knoll, W.; Koper, I. *Biophys. J.* **2005**, *89*, 1780−1788.
(9) Giess, F.; Friedrich, M. G.; Heberle, J.; Naumann, R. L.; Knoll, W. *Biophys. J.* **2004**, *87*, 3213−3220.
(10) Kim, J. M.; Patwardhan, A.; Bott, A.; Thompson, D. H. *Biochim. Biophys. Acta-Biomembranes* **2003**, *1617*, 10−21.
(11) Lingler, S.; Rubinstein, I.; Knoll, W.; Offenhausser, A. *Langmuir* **1997**, *13*, 7085−7091.
(12) Naumann, R.; Jonczyk, A.; Kopp, R.; Vanesch, J.; Ringsdorf, H.; Knoll, W.; Graber, P. *Angew. Chem., Int. Ed. Engl.* **1995**, *34*, 2056−2058.
(13) Naumann, R.; Schiller, S. M.; Giess, F.; Grohe, B.; Hartman, K. B.; Karcher, I.; Koper, I.; Lubben, J.; Vasilev, K.; Knoll, W. *Langmuir* **2003**, *19*, 5435−5443.
(14) Raguse, B.; Braach-Maksvytis, V.; Cornell, B. A.; King, L. G.; Osman, P. D. J.; Pace, R. J.; Wieczorek, L. *Langmuir* **1998**, *14*, 648−659.
(15) Silin, V. I.; Wieder, H.; Woodward, J. T.; Valincius, G.; Offenhausser, A.; Plant, A. L. *J. Am. Chem. Soc.* **2002**, *124*, 14676−14683.
(16) Terrettaz, S.; Mayer, M.; Vogel, H. *Langmuir* **2003**, *19*, 5567−5569.
(17) Wagner, M. L.; Tamm, L. K. *Biophys. J.* **2000**, *79*, 1400−1414.
(18) Kiessling, V.; Tamm, L. K. *Biophys. J.* **2003**, *84*, 408−18.
(19) Deverall, M. A.; Gindl, E.; Sinner, E. K.; Besir, H.; Ruehe, J.; Saxton, M. J.; Naumann, C. A. *Biophys. J.* **2005**, *88*, 1875−1886.
(20) Merzlyakov, M.; Li, E.; Casas, R.; Hristova, K. *Langmuir* **2006**, *22*, 6986−6992.
(21) Merzlyakov, M.; Li, E.; Gitsov, I.; Hristova, K. *Langmuir* **2006**, *22*, 10145−51.
(22) Merzlyakov, M.; Li, E.; Hristova, K. *Langmuir* **2006**, *22*, 1247−1253.

10.1021/la702147m CCC: $37.00
Published on Web 11/16/2007

membrane, respectively. These results suggest that bilayers on silicon can be integrated with conventional silicon electronics and have the potential for the development of high-throughput, lab-on-a-chip devices.

Materials and Methods

Silicon Supports. All experiments were performed on n-type silicon (111) (Montco Silicon Technologies, Inc., Spring City, PA) with a resistivity of 0.001−0.005 Ω cm. Clean hydrophilic surfaces are required for LB deposition of uniform monolayers, and the wafers were therefore cleaned in piranha solution prior to monolayer deposition. Briefly, the wafers were immersed sequentially in 2-propanol (Fisher Scientific, Assay 99.9%), acetone (J.T. Baker, Assay 99.8%), and 2-propanol, sonicating for 15 min in each solvent. Finally, the wafers were immersed in piranha etch solution: 30% hydrogen peroxide (Fisher Scientific, Assay 95.4%) and 70% sulfuric acid (Fisher Scientific, Assay 31.4%). The wafers were etched for 20 min, rinsed several times in deionized (DI) water, and finally stored at room temperature in DI water prior to formation of the bilayer.

LB Deposition of Lower Leaflet. The lipid bilayers were formed using a two-step procedure, as illustrated schematically in Figure 1. In the first step, LB deposition was used to form the lower leaflet on the silicon support. Lipids and gramicidin were premixed in chloroform to achieve a total concentration of 1 mg mL^{-1}. The lipids, 1,2-diphytanoyl-*sn*-glycero-3-phosphocholine (DPhPC) and 1,2-dipalmitoyl-*sn*-glycero-3-phosphoethanolamine-*N*-[methoxy-(polyethylene glycol)-2000] (PEG-2k) were purchased from Avanti Polar Lipids (Alabaster, AL) and used without further purification. The concentration of PEG-2k was 5.9 mol %, based on the total lipid concentration. This concentration is the estimated crossover concentration for the PEG polymer chain (i.e., the transition from the "mushroom" to the "brush" regime[23]) and corresponds to the concentration where the random PEG coils begin to come into contact with each other. Gramicidin A (Fluka) was added to the lipid solution at various concentrations from 0.001 to 0.05 mol %, based on the total lipid concentration. The gramicidin/lipid concentration in the membranes was not determined but may be lower than the ratio introduced into the trough since the aqueous solubility of gramicidin may be as high as 1 nM.[24]

A lipid monolayer with 0−0.05 mol % gramicidin was deposited on a silicon substrate by the LB method using a Langmuir trough (Model 611D, Nima Technology Ltd., Coventry, England). A clean silicon support was attached to the motor-driven stage and submerged in the subphase, 18 MΩ cm water (Milli-Q, Millipore, Bedford, MA). Lipid or lipid−gramicidin solution (25 μL) was spread dropwise at the air−water interface of the open trough (600 cm^2). After spreading, the solvent was allowed to evaporate for 15 min and then the monolayer was compressed at a barrier speed of 100 cm^2 min^{-1} to a pressure of 32 mN m^{-1}. Figure 2 shows a typical pressure−area isotherm for DPhPC, illustrating that the area per molecule at this pressure is about 110 $Å^2$. The silicon substrate was withdrawn from the trough at 15 mm min^{-1} while maintaining the pressure constant at 32 mN m^{-1}. This rate was sufficiently slow to ensure that the meniscus formed at the silicon surface remained uniform during withdrawal.

After LB deposition of the DPhPC/PEG-2k/gramicidin monolayer, the silicon wafer was assembled into a three-electrode electrochemical cell. An ohmic contact was formed on the backside of the wafer using InGa eutectic after surface oxide removal by careful application of 25% HF for 1 min.

Vesicle Fusion and Formation of the Outer Leaflet. The bilayer was completed by VF of large unilamellar vesicles (LUVs). LUVs were prepared using standard techniques,[25,26] Briefly, DPhPC and Gramicidin A (0−0.05 mol %) were combined in chloroform (99.8%, Fisher Scientific) in a flat-bottomed flask. The solvent was evaporated under nitrogen flow, and then the flask was placed in a desiccator and dried for 1 h under vacuum. The lipid−gramicidin mixture was then redissolved in 1 mL of phosphate buffered saline (PBS) and vortexed for 3 min. The lipid−protein suspension, at a concentration of 1 mg mL^{-1}, was extruded (Mini-Extruder, Avanti Polar Lipids, Alabaster, AL) 10 times through a polycarbonate membrane with a pore diameter of 100 nm (Whatman).

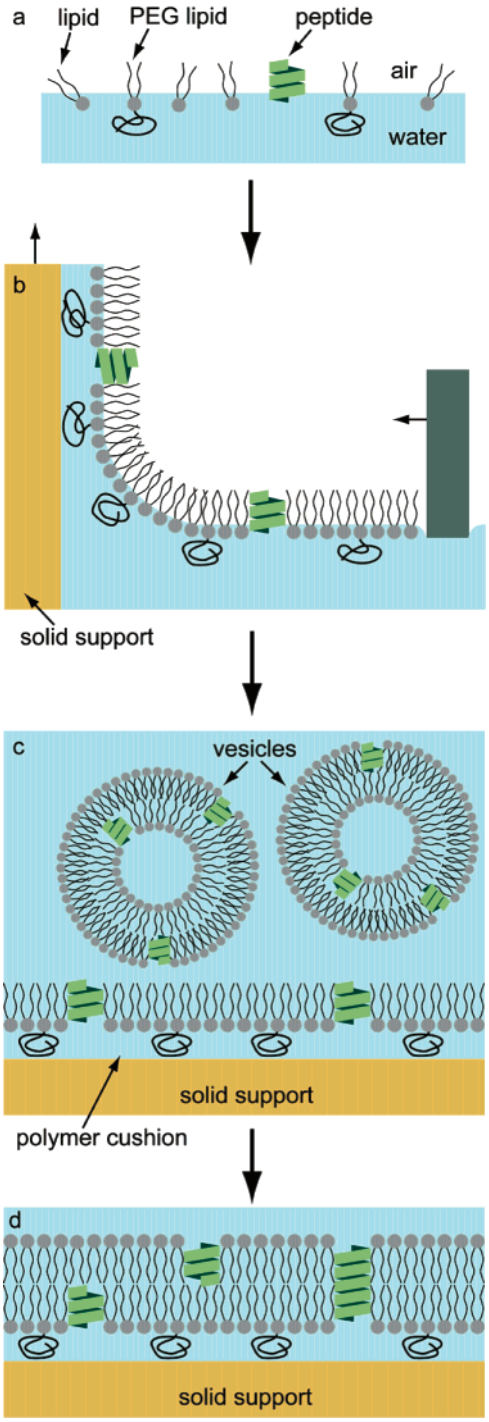

Figure 1. Schematic illustration of the formation of bilayers by Langmuir−Blodgett/vesicle fusion (LB/VF) deposition. (a) Lipids and proteins are spread on the trough, (b) deposition of the lower leaflet on the solid support, (c) vesicle fusion, and (d) formation of the upper leaflet.

(23) Kenworthy, A. K.; Hristova, K.; Needham, D.; McIntosh, T. J. *Biophys. J.* **1995**, *68*, 1921−36.
(24) Kemp, G.; Wenner, C. *Arch. Biochem. Biophys.* **1976**, *176*, 547−555.
(25) Ertel, A.; Marangoni, A. G.; Marsh, J.; Hallett, F. R.; Wood, J. M. *Biophys. J.* **1993**, *64*, 426−434.
(26) White, G.; Pencer, J.; Nickel, B. G.; Wood, J. M.; Hallett, F. R. *Biophys. J.* **1996**, *71*, 2701−2715.

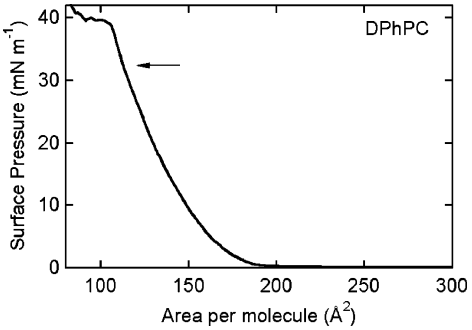

Figure 2. Pressure−area isotherm for DPhPC. Deposition was performed at 32 mN m^{-1}.

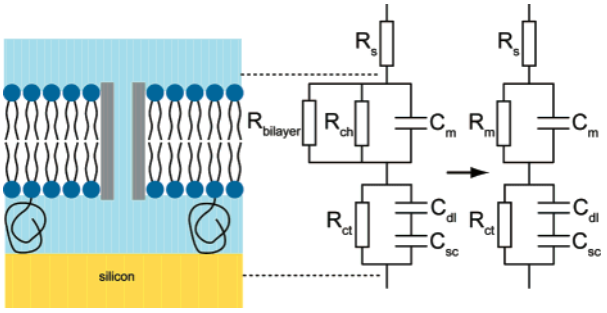

Figure 3. Schematic illustration of a supported bilayer membrane on a semiconductor support, and the equivalent circuit for the system. R_s, series resistance; $R_{bilayer}$, bilayer membrane resistance; R_{ch}, channel resistance; R_m, membrane resistance ($R_{bilayer}$ and R_{ch}); C_m, channel capacitance; C_{dl}, double layer capacitance; R_{ct}, charge-transfer resistance.

A 0.5 mL solution of the vesicles was slowly introduced into the electrochemical cell using a pipet. The bilayers were completed by incubation of the vesicles in the dark for 1 h. Prior to electrochemical measurements, additional PBS was added to a total volume of about 8 mL. All experiments were performed in 100 mM potassium phosphate buffer (sodium phosphate dibasic $Na_2HPO_4 \cdot 7H_2O$, 98−100%, J. T. Baker, NJ, and sodium phosphate monobasic NaH_2PO_4, 100%, J. T. Baker, NJ) with 100 mM KCl (99.4%, J. T. Baker, NJ), pH 6.9−7.1. All experiments were conducted at room temperature in the dark to avoid photoeffects in the silicon.

Electrochemical Characterization of Supported Bilayers. Electrochemical impedance measurements were performed with a computer-controlled potentiostat (Solartron 1286) and impedance analyzer (Solartron 1260). The electrochemical cell included a large-area platinum mesh counter electrode positioned parallel to the silicon surface and a Ag/AgCl (3 M NaCl) reference electrode ($U_{eq} = 0.200$ V vs SHE) connected to the cell via a Luggin capillary. The area of the supported bilayers for electrochemical measurements was 0.8 cm^2. All measurements were performed at an ac perturbation of 20 mV and over the potential range from 0.4 to −1.5 V. Impedance spectra were analyzed using a complex nonlinear least-squares immittance fitting program (Z Plot, Scribner Associates). All data were analyzed using an equivalent circuit with a series resistance, R_s, comprising the contacts and solution resistance, in series with two RC circuits, representing the electrical response of the membrane and the silicon electrode (see Figure 3). From the data analyses, the membrane and electrode resistance (R_m and R_{sc}) and capacitance (C_m and C_{sc}) were obtained.

Results and Discussion

Single-Crystal Silicon Support. In deconvoluting the impedance of bilayer membranes, it is important to determine the contribution of the support to the total impedance. Figure 4 shows the impedance for n-Si(111) in PBS at −0.5 V (Ag/AgCl). The Bode plot shows a high-frequency series resistance of about 40 Ω cm^2 followed by a single relaxation at lower frequencies

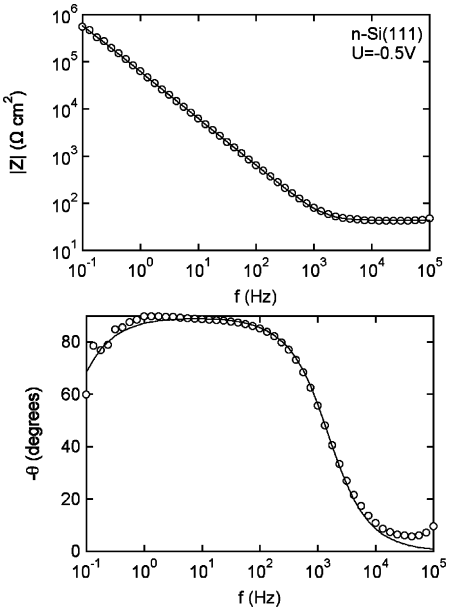

Figure 4. Experimental measurements of the impedance of n-Si-(111) in PBS at −0.5 V, (a) Bode plot and (b) phase angle. The solid lines are fits to the data using an equivalent circuit with the solution resistance, R_s, in series with a parallel RC network.

corresponding to the capacitance of the silicon/solution interface in parallel with the charge-transfer resistance.[27−30] The maximum phase angle is very close to −90°, corresponding to a near-ideal capacitor. The solid lines in Figure 4 correspond to the nonlinear least-squares fits from which we can extract the interface capacitance. Figure 5 shows that the capacitance increases from about 2 μF cm^{-2} at 0.4 V to about 4 μF cm^{-2} at −1.5 V. These values are relatively large due to the high donor density of the silicon, and hence, we cannot uniquely assign the capacitance to the space charge layer.

To resolve the contribution of the membrane in the impedance response, we must satisfy the condition that $C_m < C_{sc}$, i.e., the capacitance of the membrane must be less than the capacitance of the silicon/solution interface (see Supporting Information for details). As we show below, the capacitance of the bilayer, C_m, is about 0.8 μF cm^{-2}, providing a lower limit for the capacitance of the silicon/solution interface C_{sc}. One way to ensure that C_{sc} is sufficiently large is to use highly doped silicon for the support, since the space charge layer capacitance increases with $N_D^{1/2}$, where N_D is the donor density.

The charge-transfer resistance associated with the silicon/solution interface, as shown in Figure 5, is between 10^5 and 10^7 Ω cm^2. The impedance remains high across the measured potential range since hydrogen evolution is shifted to quite negative potentials. In our experiments at neutral pH, the equilibrium potential is about −0.6 V Ag/AgCl and the current does not increase significantly until about −1.6 V due to the large overpotential for hydrogen evolution.

DPhPC Bilayer. Figure 6 shows the magnitude and phase angle of the impedance for a DPhPC bilayer with a polymer cushion on n-Si(111) at −0.5 V (Ag/AgCl). The bilayer was formed by LB deposition of DPhPC and 5 mol % PEG-2k at 32

(27) Oskam, G.; Schmidt, J. C.; Hoffmann, P. M.; Searson, P. C. *J. Electrochem. Soc.* **1996**, *143*, 2531−2537.
(28) Oskam, G.; Schmidt, J. C.; Searson, P. C. *J. Electrochem. Soc.* **1996**, *143*, 2538−2543.
(29) Natarajan, A.; Oskam, G.; Searson, P. C. *J. Phys. Chem. B* **1998**, *102*, 7793−7799.
(30) Macdonald, D. D. *Transient techniques in electrochemistry*; Plenum Press: New York, 1977.

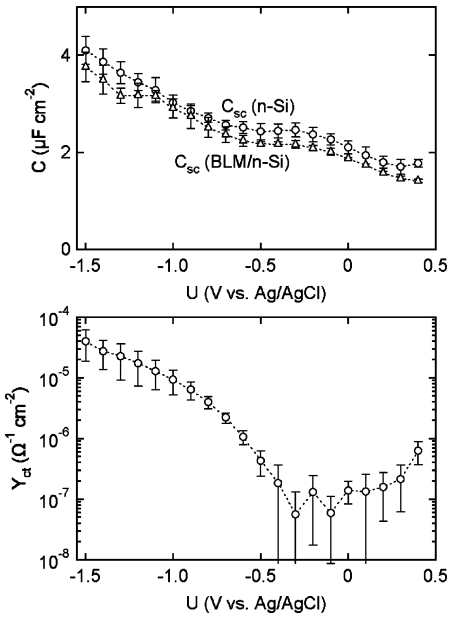

Figure 5. (Top) Capacitance versus potential plots: (○) capacitance of the silicon/solution interface obtained from impedance measurements of n-Si(111) and (Δ) capacitance of the silicon/solution interface obtained from analysis of the impedance response of DPhPC,PEG-2k/DPhPC bilayers on n-Si(111). The measured and deconvoluted values for capacitance of the silicon/solution interface overlap, indicative of robust data analysis using the equivalent circuit shown in Figure 3. (Bottom) Charge-transfer admittance, Y_{ct}, versus potential n-Si(111). Each point represents the mean and standard deviation of three experiments.

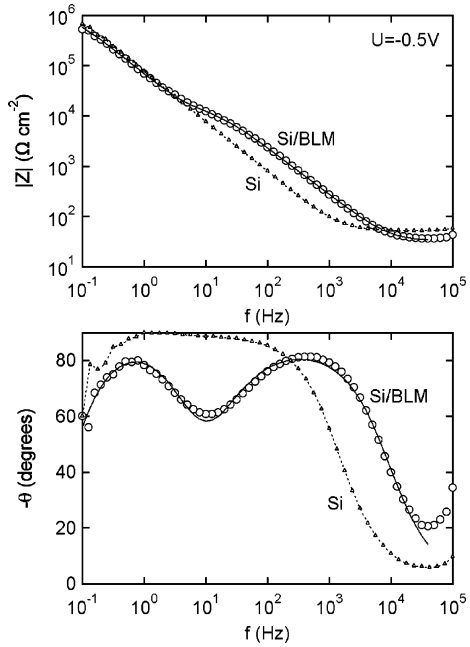

Figure 6. Experimental measurements of the impedance of a DPhPC,PEG-2k/DPhPC bilayer on n-Si(111) in PBS at −0.5 V, (top) Bode plot and (bottom) phase angle. The spectra show the same features as the simulations with the high-frequency response due to the bilayer membrane (R_m and C_m) and the low-frequency response due to the silicon support. The solid lines are nonlinear least-squares fits to the data using the equivalent circuit shown in Figure 3. The dotted lines show the impedance response of the n-Si support at the same applied potential.

mN m^{-1}, followed by fusion of DPhPC vesicles. The Bode plot shows the characteristic features of a series combination of two parallel RC networks. The higher frequency relaxation is

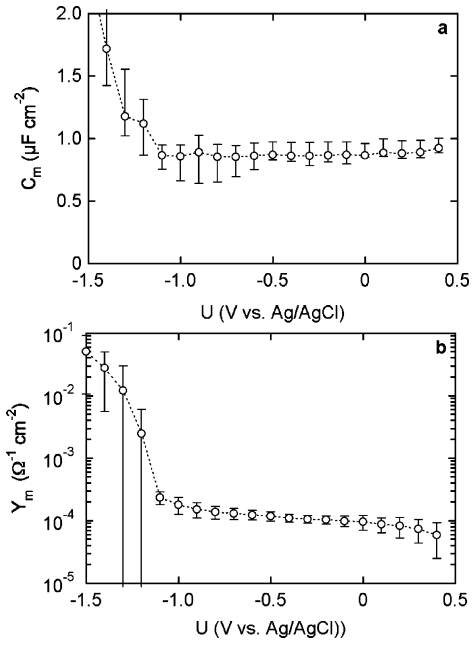

Figure 7. (a) Membrane capacitance versus potential for DPhPC,-PEG-2k/DPhPC bilayer on n-Si(111) in PBS. (b) Membrane admittance versus potential. The capacitance and admittance were determined from nonlinear least-squares fits to the complete spectrum at each potential. Each point represents the mean and standard deviation of three experiments. Both capacitance and admittance are constant over a wide potential range, from 0.4 to −1.0 V. These results demonstrate that the capacitance and admittance can be extracted from analysis of the impedance spectra using the equivalent circuit model. The relatively small standard deviation illustrates the high reproducibility of the electrical response of LB bilayers.

associated with the bilayer, and the lower frequency relaxation is associated with the space charge layer of the silicon support (see Supporting Information for details). The solid lines correspond to nonlinear least-squares fits to the spectra using the equivalent circuit shown in Figure 3 from which we can obtain the values of the circuit elements.

Figure 5 shows the potential dependence of the silicon/solution interface capacitance obtained from deconvolution of the impedance spectra for DPhPC bilayers (see Supporting Information for details). The capacitance of the silicon/solution interface obtained from analysis of the impedance spectra for the DPhPC bilayers is in excellent agreement with the values obtained from measurements of the silicon support with no bilayer in PBS, illustrating that the analysis of the impedance spectra using the equivalent circuit model in Figure 3 is robust.

Figure 7 shows the membrane capacitance C_m and membrane admittance, Y_m. Over the potential range from 0.4 to −1.0 V, $C_m \approx 0.8\,\mu$F cm^{-2}. The overall thickness of a fully hydrated DPhPC bilayer is 5.1 nm with the hydrophobic region being 2.6 nm thick.[31] Assuming a parallel plate capacitor ($C = \epsilon\epsilon_0/d$, where ϵ is the relative permittivity and ϵ_0 is the permittivity of free space), the relative permittivity of the bilayer is estimated to be in the range 2.3−4.6 (taking the limits of d as 2.6−5.1 nm), within the range of values typically reported in the literature. At more negative potentials the capacitance increases sharply toward the capacitance of the silicon/solution interface, indicating breakdown of the bilayer. Breakdown can be caused by disruption of the bilayer due to hydrogen evolution at the silicon surface or by electrical breakdown (e.g., electroporation) of the bilayer due to the high field. Assuming that most of the applied potential is dropped across the membrane and assuming that the zero

(31) Hung, W. C.; Chen, F. Y.; Huang, H. W. *Biochim. Biophys. Acta-Biomembranes* **2000**, *1467*, 198−206.

charge potential is close to the flatband potential (about 0 V (Ag/AgCl)), then the field across the bilayer (taking $d = 5$ nm) at −1.0 V is about 2×10^6 V cm^{-1}, similar to the field required to induce electroporation in mammalian cells (1×10^6−2×10^6 V cm^{-1}).[32]

The membrane admittance, also shown in Figure 7, is about 10^{-4} S cm^{-2} (an impedance of about 10^4 Ω cm^2) over the same potential range. The standard deviations of the capacitance and admittance over the potential range from 0.4 to −1.0 V are small, demonstrating that the LB deposition technique is robust and reproducible. For channel measurements, the membrane admittance is more convenient than the membrane resistance, R_m, since the admittance, Y_m, is related to the channel conductance, g_m, by $Y_m = g_{ch}n_{ch}$, where n_{ch} is the channel density in the membrane. At potentials negative to about −1.0 V (Ag/AgCl), the admittance increases sharply due to breakdown of the bilayer.

The impedances measured for tethered and hybrid bilayers are typically much larger (as high as 10^7 Ω cm^2)[5,8] than the values reported here. In order to achieve such high impedances, however, the lower leaflet is physically anchored to the support, thereby reducing or limiting the mobility of lipids and peptides. The results in Figures 6 and 7 demonstrate that LB-based deposition can be used to form supported, biomimetic bilayers with a polymer cushion on single-crystal silicon. The resistance and capacitance of these bilayers are stable and highly reproducible over a wide potential range from 0.4 to −1.0 V.

Bilayer with Gramicidin. Gramicidin is an antibiotic that functions by increasing the cation permeability of the target bacterial membrane.[33] The gramicidin monomer is a 15 amino acid, single-stranded β-helix with a molecular weight of about 2 kD where the backbone is stabilized by hydrogen bonds between carboxylic acid and amine functionalities.[33,34] Gramicidin monomers were incorporated in the lower leaflet during LB deposition and in the upper leaflet during vesicle fusion, as described in the Materials and Methods section. The cylindrical monomer has a hydrophobic exterior that is stabilized in either leaflet with the central core oriented perpendicular to the bilayer. Channels are formed by dimerization of monomer units in the upper and lower leaflet. The bilayer spanning dimeric channel is about 18 Å in diameter and 26 Å high.[35,36] The central opening is 4 Å[35,36] in diameter, resulting in permeability to small monovalent cations and water. Potassium, with a hydrodynamic diameter of about 2.5 Å, can be easily transported through the gramicidin channel.

Figure 8 shows the membrane capacitance and admittance for DPhPC bilayers with different concentrations of gramicidin. The capacitance of the membrane is about 0.8 μF cm^{-2}, independent of gramicidin concentration and applied bias. The membrane admittance is also independent of applied bias over a 1.5 V range and increases with increasing gramicidin concentration from less than 10^{-4} Ω^{-1} cm^{-2} to more than 10^{-2} Ω^{-1} cm^{-1}.

Figure 9 shows the admittance at −0.5 V versus gramicidin concentration. The admittance increases monotonically confirming that the number of dimerized gramicidin channels increases with increasing gramicidin concentration. The channel admittance is determined by subtracting the bilayer admittance ($Y_{bilayer}$ = 0.000118 S cm^{-2}) from the total membrane admittance ($Y_{ch} = Y_m - Y_{bilayer}$). If we assume that the gramicidin/lipid ratio in the membrane is the same as the ratio introduced into the trough and the same as the ratio used to prepare the vesicles, and that all

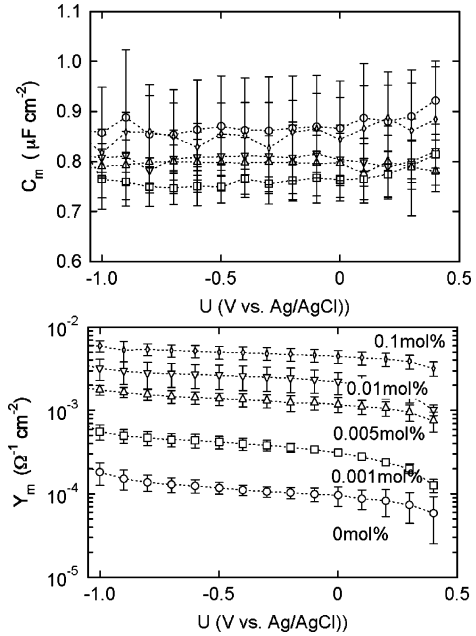

Figure 8. (Top) Capacitance and (bottom) admittance of DPhPC,-PEG-2k/DPhPC membranes versus potential for different gramicidin concentrations. Each experiment was repeated three times. The capacitance is independent of gramicidin concentration, whereas the membrane admittance increases monotonically with gramicidin concentration due to ionic conduction through the dimerized channels.

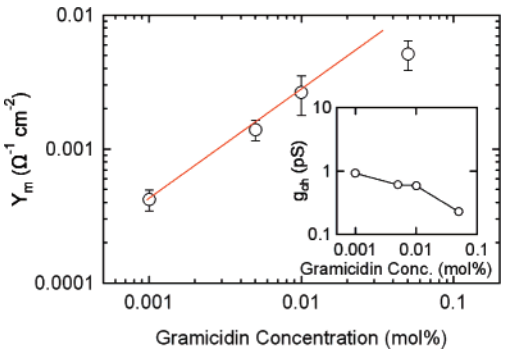

Figure 9. Admittance of DPhPC,PEG-2k/DPhPC membranes versus gramicidin concentration. The inset shows the channel conductance obtained from Y_{ch}/n_{ch} where $Y_{ch} = Y_m - Y_{BLM}$ and assuming that all gramicidin monomer is dimerized (n_{ch} = [M]/2 where [M] is the monomer concentration) using an area per molecule of 110 Å^2. As discussed in the text, the concentration of gramicidin in the bilayer is expected to be lower than the amount added due to the finite solubility in the water subphase. Thus, the conductance values are within the expected range.

gramicidin monomers are dimerized, we obtain a channel conductance ($g_{ch} = Y_{ch}/n_{ch}$) of about 1 pS, as shown in the inset of Figure 9. However, the gramicidin/lipid concentration may be lower than the ratio introduced into the trough since the aqueous solubility of gramicidin may be as high as 1 nM,[24] leading to an underestimate of the channel conductance. Furthermore, if we take into account the association constant for gramicidin (K_A = 1×10^{14} or 1.51×10^4 cm^2 mol^{-1})[37−40] the conductance increases to values in the range 1−5 pS. These values are somewhat smaller

(32) Weaver, J. C. *IEEE Trans. Dielectr. Electr. Insul.* **2003**, *10*, 754−768.
(33) Andersen, O. S. *Annu. Rev. Physiol.* **1984**, *46*, 531−48.
(34) Ketchem, R. R.; Hu, W.; Cross, T. A. *Science* **1993**, *261*, 1457−60.
(35) Koeppe, R. E.; Andersen, O. S. *Annu. Rev. Biophys. Biomol. Struct.* **1996**, *25*, 231−258.
(36) Urry, D. W.; Goodall, M. C.; Glickson, J. D.; Mayers, D. F. *Proc. Natl. Acad. Sci. U.S.A.* **1971**, *68*, 1907−11.
(37) Rokitskaya, T. I.; Antonenko, Y. N.; Kotova, E. A. *Biochim. Biophys. Acta* **1996**, *1275*, 221−6.
(38) Hladky, S. B.; Haydon, D. A. *Biochim. Biophys. Acta* **1972**, *274*, 294−312.
(39) Bamberg, E.; Lauger, P. *Biochim. Biophys. Acta* **1974**, *367*, 127−33.
(40) Schonknecht, G.; Althoff, G.; Junge, W. *J. Membr. Biol.* **1992**, *126*, 265−75.

than the values of about 10−20 pS reported in the literature for the conductance of gramicidin channels[38,41−43] but are reasonably close given the uncertainty in determining the gramicidin concentration.

In control experiments (not shown) using tetrabutyl ammonium ions ($N(C_4H_9)_4^+$, hydrodynamic diameter ≈ 9.3 Å) that are too large to be transported through the channel ($d \approx 4$ Å), the membrane admittance in the presence and absence of the gramicidin channel is similar. These results, collected for a "monolithic channel," demonstrate that the inclusion of a channel can be easily detected by impedance measurements.

Conclusions

We have demonstrated that LB deposition techniques are an alternative approach for the assembly of electrically addressable bilayer membranes with polymer cushions on semiconductor supports. The polymer cushion allows for high lipid and membrane protein mobility in both the upper and lower leaflet and also provides space for incorporation of membrane proteins that extend out of the bilayer.[17,21] While LB techniques have been used to deposit bilayers directly onto gold supports, they are expected to have limited lipid and protein mobility.[44,45] The silicon support provides integration with conventional silicon electronics and the potential for the development of high throughput, lab-on-a-chip devices.

Previous work on the characterization of membrane proteins embedded in LB bilayers on nonconducting supports has been based on fluorescence detection.[18,19,21] Here we have characterized the electrical response of bilayers produced via LB/VF deposition on silicon, and we have shown that the electrical response of the pure bilayer is robust and reproducible and that the incorporation of gramicidin alters the bilayer impedance as expected. Thus, LB bilayers on silicon can be used as platforms for investigation of ion channels. Importantly, conductance studies can be carried out in conjunction with other biophysical studies, such as studies of lateral interactions between membrane proteins and assembly of transmembrane helices into functional units. Thus, we have demonstrated that LB bilayers present a superior platform for characterization of membrane proteins.

Acknowledgment. The authors gratefully acknowledge support from NSF (grant number MCB 078841). J.L. acknowledges support from the NSF IGERT NanoBio training grant.

Supporting Information Available: Overview of the impedence response of supported bilayer membranes. This material is available free of charge via the Internet at http://pubs.acs.org.

LA702147M

(41) Rokitskaya, T. I.; Kotova, E. A.; Antonenko, Y. N. *Biophys. J.* **2002**, *82*, 865−73.

(42) Borisenko, V.; Lougheed, T.; Hesse, J.; Fureder-Kitzmuller, E.; Fertig, N.; Behrends, J. C.; Woolley, G. A.; Schutz, G. J. *Biophys. J.* **2003**, *84*, 612−22.

(43) Lundbaek, J. A.; Andersen, O. S. *J. Gen. Physiol.* **1994**, *104*, 645−73.

(44) Garcia-Araez, N.; Brosseau, C. L.; Rodriguez, P.; Lipkowski, J. *Langmuir* **2006**, *22*, 10365−10371.

(45) Zawisza, I.; Bin, X. M.; Lipkowski, J. *Langmuir* **2007**, *23*, 5180−5194.